Romanian Reports in Physics, Vol. 61, No. 4, P. 646–655, 2009

NUCLEAR PHYSICS

INERTIA FOR TWO-CENTER NUCLEAR SHAPE PARAMETRIZATIONS

M. MIREA[1], R.C. BOBULESCU[2], M. PETRE[1]

[1] *"Horia Hulubei" National Institute for Nuclear Physics and Engineering, P.O.Box MG-6, RO-077125 Bucharest-Magurele, Romania, E-mail: mirea@nipne.ro*
[2] *Faculty of Physics, University of Bucharest, P.O. Box MG-11, Bucharest, Romania*

(Received August 31, 2009)

Abstract. The effective mass is calculated in two different approaches: the Werner-Wheeler method and the cranking model. In both cases the nuclear shape parametrization is given by two spheres of different radii smoothly joined with a third toroidal surface that describes a neck. The wave functions required to compute the effective mass in the cranking model are obtained with a recent version of the superasymmetric two-center shell model that solve a Woods-Saxon potential. The difference between the results given by the two approximations are presented.

1. INTRODUCTION

In most usual theoretical treatments of nuclear fission, the whole nuclear system is characterized by some collective coordinates associated with some degrees of freedom that determine approximately the behavior of many other intrinsic variables. The basic ingredient in such an analysis is a shape parametrization that depends on several macroscopic degrees of freedom. The generalized coordinates associated to these degrees of freedom vary in time leading to a split of the nuclear system in two separated fragments. A microscopic potential must be constructed, to be consistent with this nuclear shape parametrization. It is known that a nuclear shape can be well characterized for fission processes if the following conditions are satisfied [1]: (*i*) The three most important degrees of freedom, that is, elongation, necking and mass-asymmetry, must be taken into account. (*ii*) A single sphere and two fragments should be allowed configurations. (*iii*) The flatness of the neck must be an independent variable. All these conditions will be fulfilled in the following.

In the present work, an axial-symmetric nuclear parametrization is obtained by smoothly joining two intersected spheres of different radii R_1 and R_2 with a neck surface generated by the rotation of a circle of radius R_3 around the symmetry axis, as displayed in Fig. 1. The surface equation is given in cylindrical coordinates:

$$\rho_s(z) = \begin{cases} \sqrt{R_1^2 - (z - z_1)^2}, & z \le z_{c1} \\ \rho_3 - s\sqrt{R_3^2 - (z - z_3)^2}, & z_{c1} < z < z_{c2} \\ \sqrt{R_2^2 - (z - z_2)^2}, & z_{c2} \le z, \end{cases} \tag{1}$$

where z_{c1} and z_{c2} define the region of the necking. The meaning of the geometrical symbols that depends on the shape parametrization can be understood inspecting Fig. 1. This parametrization allows to characterize a single nucleus or two separated nuclei. Throughout the paper, the subscripts 0, 1, and 2 indicate the parent, the heavy and light fragments, respectively. If S=1, the shapes are necked in the median surface characterizing scission shapes and if S=–1 the shapes are swollen characterizing the ground-state and saddle points. The generalized coordinates used in the following are denoted $R = z_2 - z_1$ (elongation), $C = S/R_3$ (necking) and $\eta = R_1/R_2$ (mass-asymmetry). For large distances between the two nascent fragments, the configuration given by two separated spheres is reached.

2. INERTIA

In a multidimensional deformation space, where the nuclear shape is described by a set of n independent generalized coordinates $\{q_i\}$ (i = 1, ..., n), the inertia tensor B_{ij} is defined by the equation of the kinetic energy T:

$$T = \frac{1}{2}\sum_{i,j=1}^{n} B_{ij}(q_1, \ldots, q_n)\frac{\mathrm{d}q_i}{\mathrm{d}t}\frac{\mathrm{d}q_j}{\mathrm{d}t}, \tag{2}$$

There are different methods of calculation of these quantities. Two of them are widely used in nuclear physics, that are, the Werner-Wheeler approximation and the cranking model.

2.1. THE WERNER-WHEELER APPROXIMATION

In the Werner-Wheeler approximation [2, 3, 4], the flow of the fluid is idealized as non-rotational, non-viscous and hydrodynamic. The effective mass can be computed within the following formula:

$$B_{ij} = \pi\sigma\int_{z_{\min}}^{z_{\max}} \rho^2(z)\left(X_i(z)X_j(z) + \frac{1}{2}Y_i(z)Y_j(z)\right)\mathrm{d}z, \tag{3}$$

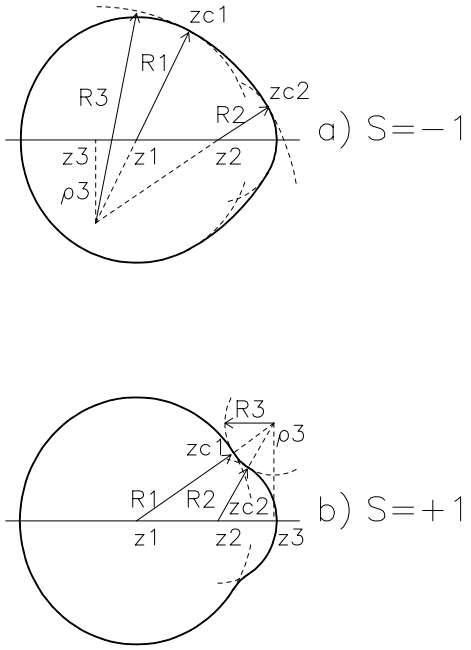

Fig. 1 – Nuclear shape parametrization. z_1, z_2 and z_3 are the positions of the centers of circles of radii R_1, R_2 characterizing the two nascent fragments, and of R_3 determining the neck, respectively. If $s = 1$, the shape is necked, otherwise the shape is swollen in the median surface. The distance between the two centers z_1 and z_2 determines the elongation R.

where $\rho_s(z)$ defines the nuclear surface and the origin of z is placed in the center of mass. z_{min} and z_{max} refer to the two ends of the nucleus along the axis of symmetry. The mass density is $\sigma = 3m/\left(4\pi r_0^3\right)$, m being the nucleon mass and r_0=1.16 fm is the radius constant. The shape dependent functions are:

$$X_{i(r)}(z) = \frac{1}{\rho^2(z)}\frac{\partial}{\partial q_i}\int_{z}^{z_{\max}} \rho^2(z)\mathrm{d}z, \tag{4}$$

$$X_{i(l)}(z) = \frac{1}{\rho^2(z)}\frac{\partial}{\partial q_i}\int_{z_{\min}}^{z} \rho^2(z)\mathrm{d}z, \tag{5}$$

$$Y_{i(r,l)}(z) = \frac{\rho(z)}{2}\frac{\partial}{\partial z}X_{i(r,l)}(z). \tag{5}$$

Formula (4) is especially useful for calculating X for values of z greater than the position of the center of mass while formula (5) addresses values of z lower than the center of mass position.

2.2. THE CRANKING MODEL

In the adiabatic description of the collective behavior of a nucleus, the nucleons are assumed to move in a average deformed potential. Using a Hamiltonian that includes pairing interactions, introducing the collective parameters q_i by means of the Lagrange nultipliers, it is possible to obtain the response of the nuclear system for slow changes of the shape from the cranking model formula:

$$B_{ij} = 2\hbar^2 \sum_{\nu,\mu} \frac{<\mu|\partial H/\partial q_i|\nu><\nu|\partial H/\partial q_j|\mu>}{\left(E_\mu + E_\nu\right)} \cdot \cdot \left(u_\nu v_\mu + u_\mu v_\nu\right)^2 + P_{ij}, \tag{7}$$

where H is the single-particle Hamiltonian, $|\nu>$ and $|\mu>$ are single particle wave functions, E_ν, u_ν and v_ν are the quasiparticle energy, the vacancy and occupation amplitudes of the state ν, respectively, in the BCS approximation, and P_{ij} is a correction that depends on the variation of the parameters Δ (the pairing gap) and λ (the Fermi energy) as function of deformations. The total inertia is the sum of the partial values that correspond to protons and neutrons. Detailed explanations are given in Refs. [5, 6]. Usually, the matrix elements of the derivatives of the Hamiltonian are replaced by the matrix elements of the derivatives of the potential. In this paper, the Rel. (7) will be used to compute the cranking inertia in terms of the Woods-Saxon superasymmetric two-center shell model [7, 8]. This model was already used to determine the fusion probability for the formation of superheavy elements [9]. This version of the two center shell model includes a realistic treatment of the dependence of the spin orbit operator in the region of the neck that cannot be achieved within the modified two-center oscillator [10, 11, 12]. This behavior was evidenced in Ref. [13] where the experimental heights of the double fission barrier are very well reproduced. Other recipes to solve a Woods-Saxon potential in a two center basis are given in Ref. [14, 15].

3. RESULTS

The effective mass will be computed for fission processes. As in Ref. [16], one of the most probable partition in the fission process of $^{233}\mathrm{Th} \rightarrow {}^{98}\mathrm{Sr} + {}^{135}\mathrm{Te}$ is

selected. In this case, the heavy fragment issued in this reaction is almost spherical, while the light one is little deformed, allowing a description in terms of our nuclear shape parametrization.

A way to obtain the sequence of nuclear shapes available for fission is to use the least action principle [6]. It is very difficult to treat the three independent generalized coordinates in the same time in order to minimize the action integral. Some simplifying assumptions must be introduced. As mentioned also in Ref. [17], microscopic approaches to fission [18, 19] established that the second saddle point is asymmetrical with a value compatible with the observed mass ratio. In the same time, in the region of the second barrier, the mass-asymmetry component of the inertia tensor is very large [20]. So, the variations of the mass-asymmetry generalized coordinate are hindered in this region. On another hand, for elongations smaller than that of the outer barrier, the mass-asymmetry component of the inertia is much lower. Therefore, up to the second barrier top, the mass-asymmetry coordinate can be modified without enhancing too much the value of the action integral. Moreover, even the deformation energy is less sensitive to variations of the mass-asymmetry coordinate in the region of compact shapes. As in Ref. [20], this observation allows us to reduce the number of parameters in order to rend our problem tractable. Therefore, the evolution of the mass asymmetry generalized coordinate will be a priori fixed in the following. It is assumed that the ratio $\eta = R_1 / R_2$ varies linearly from unity (first barrier top) to the value associated with the final mass partition (second barrier top). The mass asymmetry in the outer barrier region is deduced by considering that the volume occupied by the light fragment equals the final one.

Along the trajectory, the inertia can be reduced to:

$$B = B_{RR} + B_{CC}\left(\frac{\partial C}{\partial R}\right)^2 + B_{\eta\eta}\left(\frac{\partial \eta}{\partial R}\right)^2 + 2B_{RC}\frac{\partial C}{\partial R} + 2B_{R\eta}\frac{\partial \eta}{\partial R} + \\ + 2B_{C\eta}\frac{\partial C}{\partial R}\frac{\partial \eta}{\partial R}, \tag{8}$$

where B_{RR}, B_{CC} and $B_{\eta\eta}$ are the diagonal components along the three independent collective degrees of freedom and B_{RC}, $B_{R\eta}$ and $B_{C\eta}$ are the offdiagonal components. If the variation of the mass-asymmetry is apriori determined, then the inertia tensor has only three components:

$$B_{\text{ELONGATION}} = B_{RR} + B_{\eta\eta}\left(\frac{\partial \eta}{\partial R}\right)^2 + 2B_{R\eta}\frac{\partial \eta}{\partial R}, \\ B_{\text{NECK}} = B_{CC}, \tag{9} \\ B_{\text{ONNDIAGONAL}} = B_{RC} + B_{C\eta}\frac{\partial \eta}{\partial R},$$

because the derivative $\partial\eta/\partial R$ is known by the variation imposed to η and

$$B = B_{\mathrm{ELONGATION}} + B_{\mathrm{NECK}}\left(\frac{\partial C}{\partial R}\right)^2 + 2B_{\mathrm{ONNDIAGONAL}}\frac{\partial C}{\partial R} \tag{10}$$

becomes the inertia along the trajectory. A similar attack of the multidimensional problem has been employed in Refs. [20, 21, 22].

In Figs. 2, 3, 4, the quantities $B_{\mathrm{ELONGATION}}/\mu, \log\left(B_{\mathrm{NECK}}/\mu\right)$ and $\log\left(B_{\mathrm{OFFDIAGONAL}}/\mu\right)$ are represented in a two-dimensional configuration space spanned by the R and C generalized coordinates. The results concerning both models are displayed. Some general trends can be evidenced. The symbol μ denotes the reduced mass after scission. In these pictures, the inertia elements for the family characterized by a fixed variation of the mass-asymmetry shape parameter are displayed, as discussed previously, but the emerging observations are valid for any mass-asymmetry. Low values of $B_{\mathrm{ELONGATION}}$ are obtained for small C-values. That means, a higher probability to penetrate the barrier can be obtained for swollen shapes. On the other hand, very large values of B_{NECK} and $B_{\mathrm{OFFDIAGONAL}}$ are found exactly in the region of swollen shapes. This behavior suggests that in the region of swollen shapes, the nuclear system must evolves with a fixed value of the neck generalized coordinate in order to have very small values of $\partial C/\partial R$. Also, large values of the inertia are displayed in the vicinity of the scission points. The huge values of the inertia in the scission region are mainly due to the mass-asymmetry components. That means, the process of changing the mass-asymmetry in the vicinity of the scission is hindered.

In Fig. 2, the variations of the diagonal component $B_{\mathrm{ELONGATION}}$ of the inertia divided by the reduced mass are plotted as function of the elongation and the neck parameter. The upper panel is obtained within the Werner-Wheeler method while the lower one is given in the cranking framework. For positive values C, the nuclear system is necked in the median region, while for negative values the nuclear shapes are swollen. For positive C and large values of R, the scission is produced. The Werner-Wheeler method predicts very large values of the inertia in the region where the scission is produced (R=22 fm, C=0.2 fm^{-1}) while in the frame of the cranking approximation the values are much lower. After scission, the Werner-Wheeler method gives a inertia that corresponds to the reduced mass while the cranking approximation gives a value 1.4 times larger. In the region of swollen shapes, that describes the ground state, the inertia obtained within the cranking model is up to 10 times larger than that obtained within the irrotational approximation. Large fluctuations are obtained in the frame of the cranking model. In Fig. 3, the variations of B_{NECK} are plotted. In this case, the two approaches give a similar behavior, that is, the inertia increases strongly in the vicinity of the region where the scission is produced. After scission, this component of the inertia tensor

reaches zero. In Fig. 4, the off-diagonal component of the inertia is plotted. After scission this component becomes zero. The values obtained in the two approximations are not very different but some fluctuations can be observed in the lower panel.

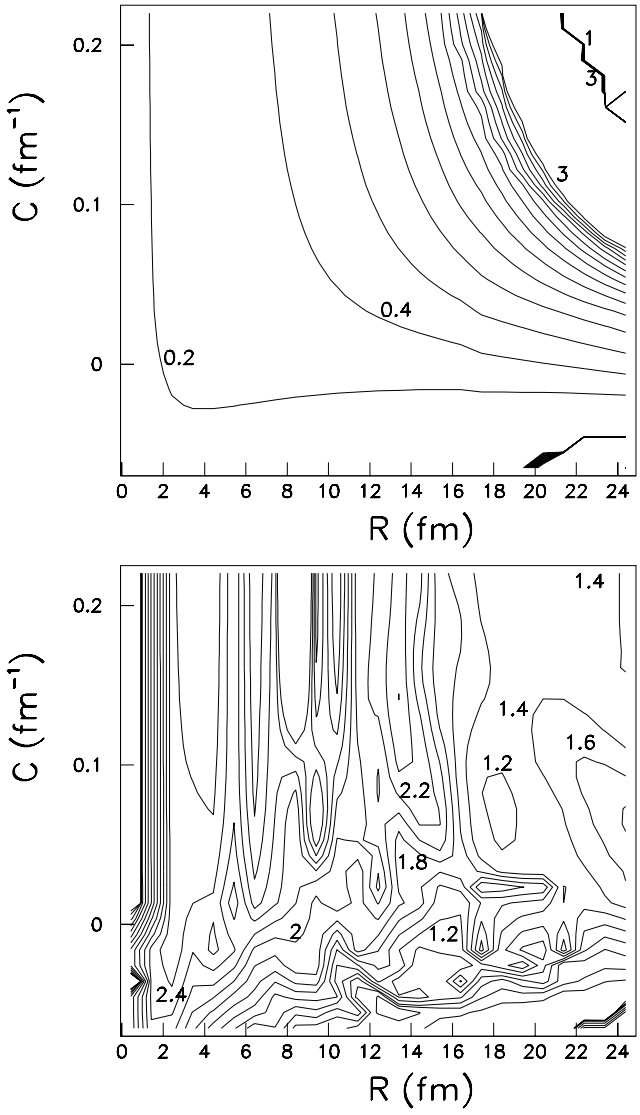

Fig. 2 – The 236U $B_{\mathrm{ELONGATION}}/\mu$ diagonal element of the inertia tensor for reflection–asymmetric nuclear shapes in the (C, R) plane. $\mu = A_1A_2/A_0$ is the reduced mass of the system. $B_{\mathrm{ELONGATION}}/\mu$ is dimensionless. The difference between two contour values is 0.2. The upper plot addresses the Werner-Wheeler approximation while the lower one concerns the cranking model. Several values are plotted on the plots.

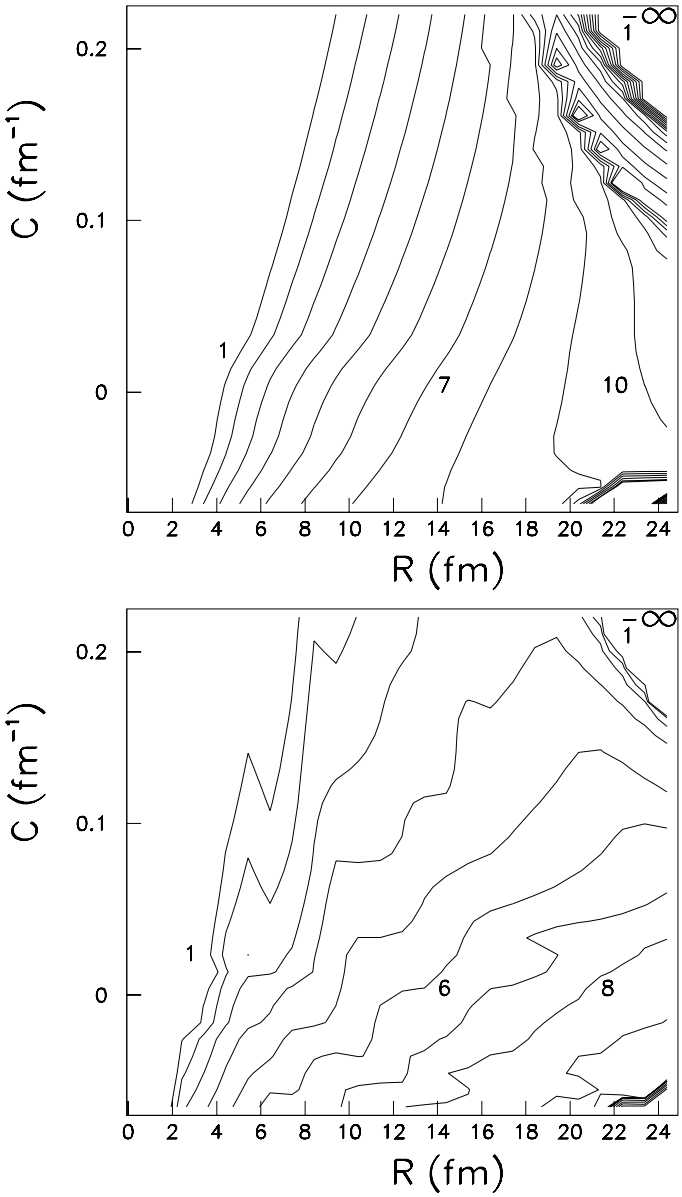

Fig. 3 – The ^{236}U log(B_{NECK}/μ) diagonal element of the inertia tensor for reflection–asymmetric nuclear shapes. The dimension of B_{NECK}/μ is fm4. The di_erence between two contour values is one unit. The upper plot addresses the Werner-Wheeler approximation while the lower one concerns the cranking model. Several values are plotted on the plots.

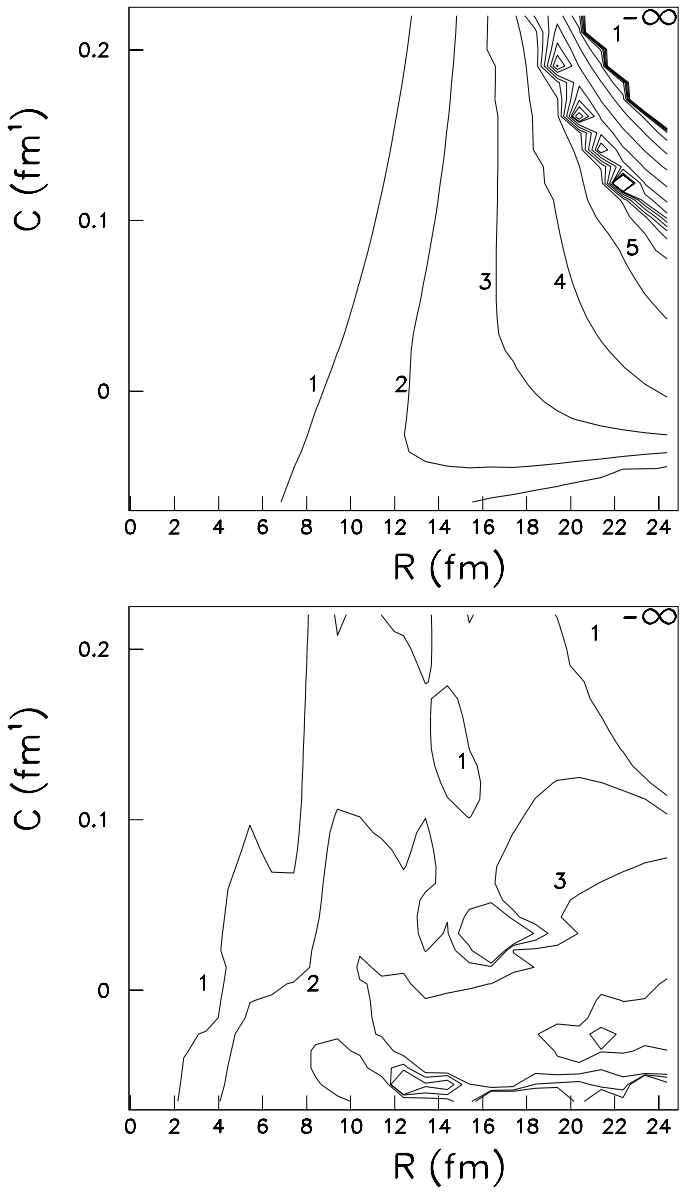

Fig. 4 – The ^{236}U log($B_{\mathrm{OFFDIAGONAL}}/\mu$) off–diagonal element of the inertia tensor for reflection–asymmetric nuclear shapes. The dimension of $B_{\mathrm{OFFDIAGONAL}}/\mu$ is fm2. The difference between two contour values is one unit. The upper plot addresses the Werner-Wheeler approximation while the lower one concerns the cranking model. Several values are plotted on the plots.

In conclusion, the inertia is computed in the frame of the cranking approach using for the first time the two-center Woods-Saxon model. The model succeeded to reproduce approximately the reduced mass of a fissioning system. A comparison within the irrotational flow model was realized and the main differences between the two approaches are emphasized.

Acknowledgments. This work was supported in the frame of the IDEI 512 program of the Romanian Ministry of Education and Research.

REFERENCES

1. U. Brosa, S. Grossman and A. Muller, Phys. Rep., **197**, 167 (1990).
2. K.T.R. Davies, A.J. Sierk and J.R. Nix, Phys. Rev. C, **13**, 2385 (1976).
3. M. Mirea, D.N. Poenaru and W. Greiner, Nuovo Cimento A, **105**, 571 (1992).
4. M. Mirea, D.N. Poenaru and W. Greiner, Z. Phys. A, **349**, 39 (1994).
5. M. Brack, J. Damgaard, A.S. Jensen, H.C. Pauli, V.M. Strutinsky, C.Y. Wong, Rev. Mod. Phys., **44**, 320 (1972).
6. T. Ledergerber, H.C. Pauli, Nucl Phys. A, **207**, 1 (1973).
7. M. Mirea, Rom. Rep. Phys., **59**, 523 (2007).
8. M. Mirea, Phys. Rev. C, **78**, 044618 (2008).
9. M. Mirea, D.S. Delion and A. Sandulescu, EPL, **85**, 12001 (2009).
10. M. Mirea, Phys. Rev. C, **54**, 302 (1996).
11. M. Mirea, Nucl. Phys. A, **780**, 13 (2006).
12. M. Mirea, R.C. Bobulescu and E. Petrescu, Rom. J. Phys., **52**, 15 (2007).
13. M. Mirea and L. Tassan-Got, Rom. J. Phys., **54**, 331 (2009).
14. A. Diaz-Torres and W. Scheid, Nucl. Phys. A, **737**, 373 (2005).
15. A. Diaz-Torres, Phys. Rev. Lett., **101**, 122501 (2008)
16. M. Mirea, L. Tassan-Got, C. Stephan, C. O. Bacri, and R.C. Bobulescu, Phys. Rev. C, **76**, 064608 (2007).
17. J.P. Bocquet and R. Brissot, Nucl. Phys. A, **502**, 213c (1989).
18. J.F. Berger, M. Girod and D. Gogny, Nucl. Phys. A, **428**, 23c (1984).
19. P. Moller, A. Iwamoto, Phys. Rev. C, **61**, 047602 (2000).
20. M. Mirea, L. Tassan-Got, C. Stephan and C.O. Bacri, Nucl. Phys. A, **735**, 21 (2004).
21. M. Mirea, L. Tassan-Got, C. Stephan, C.O. Bacri, P. Stoica and R.C. Bobulescu, J. Phys. G, **31**, 1165 (2005).
22. M. Mirea, L. Tassan-Got, C. Stephan, C.O. Bacri and R.C. Bobulescu, Europhys. Lett., **73**, 705 (2006).